UDC 543

Concentration waves behavior and the chromatographic displacement development in the sorbents-nanocomposites during the multicomponent mass transfer and visualization of the sorption kinetics process

Kalinitchev A.I.

Frumkin Institute of Physical chemistry and Electrochemistry Russian academy of sciences (IPCE RAS), Moscow

Received 26.01.2019

DOI: 10.17308/sorpchrom.2019.19/1166

There is considered the Multi-(6^{th})-component Mass Transfer (MMT) inside the planar matrices of the sorbent-NanoComposite (NC) by the computerized modelling. During the MMT kinetics in the NC planar-membrane the chromatographic Displacement Development (DD) for the propagating modes of the two concentration $X_{m(1,2)}$(L,T)-principal waves is modeled for the two principal $m_{1,2}$-sorbate components (m=1,2) of the Multi(6)-components NC MMT combined «Diffusion, and sorption» system.

The computerized modelling mentioned here is based on the mathematical solution of the MMT multi 6-components Eqns. partial differential including as the basis the author's bi-functional NC MMT Models. The main advantage of the NC Models considered concludes in the introduction of the two sorbate diffusing principal $P_{i(3.4)}$-components into the consideration. The similarity and the differences between the multicomponent X_n(L,T)-concentration waves propagation for the MMT processes in the modern NC matrix and in the chromatographic column are discussed.

The visualization of the kinetics of the MMT процесс is realized by the creation of the Sci. computerized Animations: «SCA.avi» video-files which demonstrate visually (after the program start) the propagation of the multi(n)-component $X_{n(1-6)}$(L,T)-concentration waves through the NC matrixe. Here the «SCA.avi» animations display the DD chromatographic effect during oral presentation with the mentioned DD-displacement of the X_2-concentration waves by the X_1- waves of the 1-component (displacer).

Keywords: NanoComposites(NC); Multicomponent Mass Transfer (MMT);Selectivity, Multi-Diffusion Concentration Waves; Bi-Functionality; Active Nano-Sites, , particular Chromatographic Waves

Поведение концентрационных волн и хроматографическое вытеснение в сорбентах-нанокомпозитах в течение многокомпонентного массопереноса и визуализация кинетического процесса

Калиничев А.И.

Институт физической химии и электрохимии РАН им. А.Н. Фрумкина, Москва

В работе изучается много(6)-компонентный массо-перенос (ММП) в планарной матрице сорбента-Нано-Композита (НК) путем компьютерного моделирования кинетического процесса ММП в НК мембране. Для принципиальных (целевых) $m_{1,2}$-компонентов сорбата (m=1,2) моделируется на компьютере вытеснительное распространение в НК двух взаимодействующих концентрационных

$X_{m(1,2)}(L,T)$-волн упомянутых 1,2-компонентов в ММП НК комбинированной системе (Диффузия и Селективная сорбция).

Визуализация кинетического ММП процесса осуществляется путем создания научных компьютерных НКА анимаций: «НКА.avi» видео-файлов, которые демонстрируют визуально распространение концентрационных $X_{\mathbf{n}(1-6)}(L,T)$-волн в среде НК. Анимации («НКА.avi») при запуске в устных докладах-презентациях демонстрируют упомянутый эффект вытеснения распространяющейся X_2-волны концентрационной X_1- волной 1-вытеснителя за счет большей величины K_S^1-селективности в матрице НК: $K_S^1 > K_S^2$ (хроматографический вытеснительный эффект).

Ключевые слова: нанокомпозиты, мультиомпонентнй массоперенос, селективность, мультидиффузионные концентрационные волны, бифункциональность, активные наносита, специфические хроматографические волны.

Introduction/Background

In the result of the mathematical computerized approach there are calculated the 6-components $X_{\mathbf{1-6}}(L,T)$ concentrations waves which propagate in the course of T(time) across the NC membrane during the combined kinetics MMT process (I, selective sorption and II, multicomponent Diffusion) [1-8]. The six(6)-components of the combined MMT-NC system includes the four interactive ionic components: $P^+_{i(3,4)}$ -sorbate and the corresponding $({}_k\mathbf{R}^0P_i)^+_{m(1,2)}$-sorbent $m_{(1,2)}$-complexes (including the fixed ${}_{k(6)}\mathbf{R}^0$-nanosites together with the concomitant $\boldsymbol{j}_5^-$-co-ions which diffuse only in the pores of the NC matrix (Fig. 1b, below). The two principal diffusing sorbate $P_{i(3,4)}{}^+$-components are transformed into the fixed state as the principal fixed $({}_6\mathbf{R}^0P_i)^+_{m(1,2)}$–«complexes», where m=1,2 (Fig.1b, and Fig. 2, below). The transformation of the two $P^+_{i(3,4)}$-sorbate components into the two principal $({}_k\mathbf{R}^0P_i)_m{}^+$-components-«complexes» is described by the MAL_S (Mass Action Law) relations (3),(4) (see Figs**.** 1**,** and Fig**.**2, *below*).

The enlarged $\mathbf{k}^{(2)}$=6-*variance* (which is definited as *number of the degree of freedom*) is the integral parameter belonging to the combined MMT NC system considered here (see [1-4]). The NC MMT combined system (I route-selective sorption and route II-Diffusion, Fig.1b) [1-8] gives the new possibility to investigate the mentioned chromatographic Displacement Development (DD) effect obtained for the NC bi-functional NC matrix (Figs 1a,b) for the two interactive and propagating $X_{m(1,2)}$-concentration waves for the two principal $({}_k\mathbf{R}^0P_i)^+_{m(1,2)}$ -components-complexes (formed due to the pair of the «association-dissociation» (1),(2)-reactions) (Fig. 1b, and 2, S below.2).

Thus the main purpose of the manuscript is the investigation of the DD-chromatographic effect for the two $X_{m(1,2)}$- interactive concentration waves which is achieved here by the computerized mathematical modelling with the proper approach on the basis of the advanced NC *bi-functional* combined Model (see illustrations at Figs 1, and Fig.2, below) with the two corresponding MMT I,II-routes (Figs.1b,and 2), namely **I**, MMT route with the two component $\{K_S^1;K_S^2\}$-Selectivity factor together with the, **II**-MMT multi-Diffusion route characterizing by the $\{\mathbf{D}_{3-5}\}$-multi-Diffusion factor [1-8].

In other words the chromatographic displacement behaviour (i.e. the DD -effect) for the two principal concentration $X_{1,2}(L,T)$ waves-profiles, occurs for the two principal $m_{(1,2)}$-components-complexes which propagate across the NC L-membrane (shown in Figs.1b by horizontal arrows) in the course of T-time. Thus there is the straight clear analogy with the displacement behaviour for the propagation of the two $X_{1,2}(L,T)$-concentration waves between the MMT selective processes in the chromatographic column and for the MMT process in the planar NC L-matrix of the L-NC membrane here. However at the NC MMT combined selective (I)-process there is the definite differences concerning the $X_{1,2}(L,T)$- waves behaviour which are emphasized here later (see S. 3,4).

The methods of the *visualisation* of the MMT NC process across the L-membrane is realized via the particular $X_{m,\mathbf{k}}(L,T)$-concentration waves behavior [1-10]. The presenta-

tion of the MMT-NC process is similar to the MMT in the multicomponent preparative frontal chromatography. The visual demonstration of the modeled $X_{1,2,6}$-concentration waves behavior will be shown (Figs. 3.4, S.4 below) via the calculated frames-pictures which are displayed in the course of Time (T^1,T^3) for the combined sorption NC MMT process.(Figs. 2-4 S.4 *below*).

The results of the generalized theoretical investigation of the selective sorption plus Multi-component MMT across the NC planar L-membrane are presented on the basis of the recent advanced *bi-functional* NC Model with the enlarged $\mathbf{k}^{(2)}(6)$- *variance* (see Figs. 1a,b; and 2). The results of the author's computerized calculation for the propagation of the multi (n=6)-component $X_{n(1-6)}$-waves in the NC-MMT kinetic process are demonstrated in the course of T-time at (see Figs. 3A,4B, S4, below).

The results of the computerized modelling for the NC-MMT $\mathbf{k}^{(2)}(\mathbf{6})$-component process are displayed visually by the pictures illustrating the $X_{\mathbf{1,2}}$ (L,T) concentration dependences for the selective chromatographic Displacement Development effect (DD) in the course of T^1,T^3-times (see Figs. 3A,4B; S.4). The DD-interaction of the propagating $X_{\mathbf{m(1,2)}}(L,T)$-concentration waves for the two principal $m_{1,2}$- sorbed components, namely $({}_k\mathbf{R}^0P_i)^+_{m(1,2)}$ -complexes into the planar NC matrix of the L-membrane taking into account a number of the determining parameters for the combined MMT NC process, namely, two component Selectivity$\{K_S^1,K_S^2\}$ factor ($I_{1,2}$ -route) and the input $\{X_{\mathbf{n}}^0\}$-concentrations values (n=1,2,…6), including the multi-component $\{\mathbf{D}_{3\text{-}5}\}$-diffusion factor(**II**, multi($D_{3\text{-}5}$)Diffusion route)[1-8].

The modern advanced **n**(6)-component MMT bi-functional Model (with $\mathbf{k}^{(2)}$=**6**-*variance*) is used during the computerized modeling of the MMT-NC combined kinetics through the bi-functional NC L-matrices (Figs. 1a,b and 2 [1-8]).

Bi-functional NC model for advanced, MMT system with $\mathbf{k}^{(2)}$-multivariance

The two travelling ionic $P_{(3.4)}^+$-principal sorbate components (with the two $\mathbf{D}_{3,4}$-diffusivities) are included into the MMT-NC process consideration inside the selective sorption **NC** matrix of the planar L-membrane. Due to the two MAL_S *association-dissociation* reactions **I,**(1),(2) the two diffusible $P_{(3.4)}^+$-principal components ($D_{(3,4)}>0$) compose the two fixed $({}_k\mathbf{R}^0P_{(3.4)})^+_{m(1,2)}$ -complexes during the combined MMT process through the NC L-matrix (Figs. 1a,b)[1-8].

The two $({}_k\mathbf{R}^0Pi)^+_{m(1,2)}$-complexes are in diffusible and therefore possess the zero Diffusivities (Diffusion coefficients), i.e. $D_{m(1,2)}=0$ (Figs. 1a,b), ${}_k\mathbf{R}^0 + P^+_{i(3)} \leftrightarrow ({}_k\mathbf{R}^0P_i)^+_{m1}$

$m_1=1$, i=3, k=6 ; (1)

${}_k\mathbf{R}^0 + P^+_{i(4)} \leftrightarrow ({}_k\mathbf{R}^0P_i)^+_{m2}$ $m_2=2$, i=4, k=6 ; (2)

including the corresponding MAL_S relations (Fig.2, up to the *left* below)

$K_S^{1,2} = [{}_k\mathbf{R}^0Pi]_m/([{}_k\mathbf{R}^0]\,[P_i])$, $m_{1,2}= 1,2$; i=3, 4 ; $\mathbf{k}^{(2)}$=6 (3-4)

Where [P*i*], $[{}_k\mathbf{R}^0Pi]_m$, $[{}_k\mathbf{R}^0]$, [P*i*] are concentrations of the n-components (see also Fig.2) [1,2].

Due to the two component MAL_S Selectivity $\{K_S^1;K_S^2\}$-factor in (3), and (4) it takes place the Displacement Development (DD) behaviour for the propagating modes of the two particular $X_{1,2}$(L,T)-principal concentration waves (Figs.3A,4B, S.4 *below*). The combined MMT-NC kinetics process for the all **n**-components (Figs.3,4) (where $\mathbf{n}=m_{(1,2)}$; P*i*(3,4); j_5, $k^{(2)}$=6) occur through the selective NC-sorbent. The kinetics processes with the advanced NC Model in the course of T-time is considered theoretically by the author's computerized modelling. The advanced computerized investigation is based on the fundamentals of the thermodynamics of the irreversible processes. [1-8, 10-13].

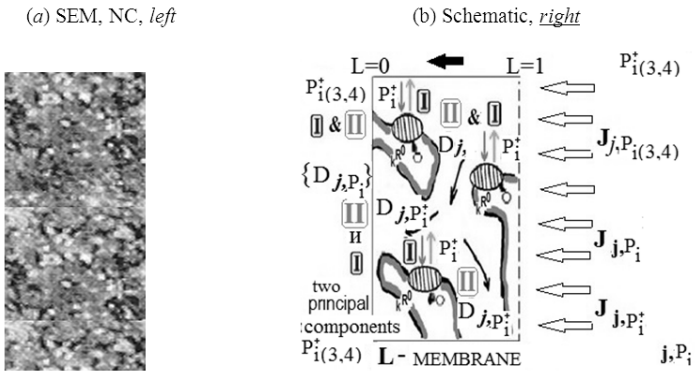

Fig. 1. (*a*, left,; b, right)(enlarged). Nanocomposite (NC) Membrane–media for the MMT kinetics process: (a)-SEM vicrography(of NC matrix, Fuji-CS(Japan), Metall^0=Ag^0[9]; (b)-principal scheme [1-8], $J_{j5,i(3,4)}$-external mass fluxes(white arrows), black arrow-direction of MMT inside NC L-matrix; MMT routes: $I_{1,2}$-selective&II-Diffusion, $Dj,_P$- D_{3-5} –Diffusivities(see Figs.3,4), principal $P^+_{i\,(3,4)}$–diffusing components, $J_{5,i(3,4)}$-external mass fluxes; I, vertical arrows(sink-source mechanism, see Fig.2),$_kR^0$-key component(«nano-sites» including sink-source mechanism) Magnification: 10000 : reactions (1), and (2) along MMT Route $\mathbf{I}_{1,2}$

The aim of this publication is to consider the generalized theoretical approach including the fundamental aspects of the Multicomponent Mass Transfer (MMT) for the sorption kinetics in the various *bi-functional* NC matrices of the selective **I**, sorption-desorption (Fig. 2) and II, multiDiffusion{D_{3-5}} for NC modern materials: **N**ano-**C**omposites (see [1-8] also).

Figures 1a,b, and 2 display the visual schemes of the bi-functional **NC** Model proposed [1-8] with the explanation of the *bi-functionality* for the NC matrices during the MMT kinetics process. There are included the two functions of the MMT NC Model considered [1-8]: (***1***)selective **I-«**route» with the *two* «adsorption(**I***a*)-desorption(**I***d*)» stages of the reactions (1),(2) (Fig. 2, up, *left*) including the two component {K_S^1,K_S^2}-Selectivity MAL_S factor (3); (4) (Fig. 2, down, *right*) for the two principal diffusing $P^+_{i(3,4)}$ -components (Figs.1a,b**,** and Fig**.** 2). In addition Fig. 1b display the second, **II**-Diffusion route for the multi-Diffusion transport characterizing by the multi-Diffusion, {D_{3-5}}-factor (see $D_{\mathbf{n}=3,4,j5}$-values at the the Figs. 3,4 of the selective combined MMT $\mathbf{k}^{(2)}$(**6**)-NC system.

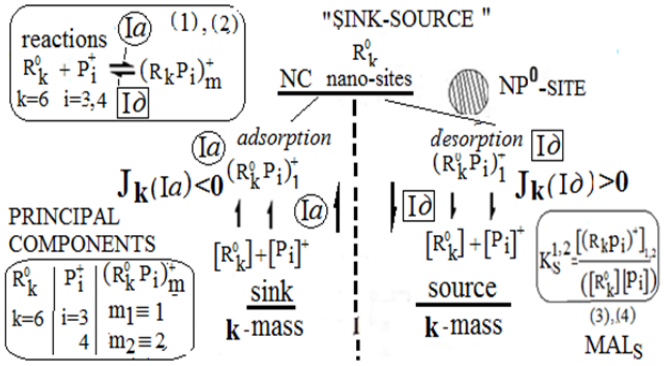

Fig.2. Sink-Source mechanism with corresponding J_k(I*a*)&J_k(Ib)-mass flaxes for *a*dsorption(I*a*)(*left*)-*d*esorption(I*d*)(*rigt*)MAL_S stages; (1),(2)-reactions(up, *left*); (3),(4)-MAL_S relations(down, *right*); fixed principal R_k^0-key (D_k=0) component («nano-sites») including «sink(*left*)-source (*right*)» MMT mechanism), R_k^0,$P^+_{i(3,4)}$, $(_kRP_i)^+_{m(1,2)}$ –principal $m_{1,2}$-components($D_{m(1,2),6}$=0), D_{3-5}>0.

In the considered MMT NC process the three components {$D_{3,4,j5}$>0}-Diffusion factor includes the two ($D_{3,4}$) - diffusing principal $P^+_{i\,(3,4)}$-(sorbate) components. Besides the accompanying j_5^-co-ions D_{j5}-**D**iffusion is included into the consideration here for the new advances MMT NC $\mathbf{k}^{(2)}$(**6**)-selective combined: **I**, selective sorption and **II**, multi-Diffusion-NC system.

The computerized modeling of the **NC**-MMT process here includes as the basis, the combined advanced *bi-functional* **NC** Model considered for the **n**(1,2,…**6**)-components in the NC MMT kinetics system with the $\mathbf{k}^{(2)}$(**6**)-*variance* (where **n**=1,2,.. ,5, $\mathbf{k}^{(2)}$=**6**). Besides $\mathbf{k}^{(2)}$(**6**) is the *variance* for the **NC- I**, selective sorption (1),(2) and **II**, multi-Diffusion selective system, which contains the two diffusing, and interactive $P^{+}_{i(3,4)}$-(sorbate) components with the corresponding two $D_{3,4}$-**D**iffusion coefficients (see Fig.1b,*above* 3,4 *below*).

According to the advanced *bi-functional* NC Model used here the two principal diffusing $P^{+}_{i(3,4)}$ sorbate components are transformed into the fixed state as the fixed $({}_{k}\mathbf{R}^{0}P_{i})^{+}_{m(1,2)}$–«complexes» (where $D_{m(1,2)}$=0). The principal $m_{(1,2)}$–components-«complexes» are in diffusible with the zero coefficients, $D_{m(1,2)}$=0, (see Figs. 1b, and Figs. 2-4). The *forward* process (**I***a*) of the «association» of the principal two diffusible $P^{+}_{i(3,4)}$-components takes place with the transformation $P^{+}_{i(3,4)}$ into the two associated $({}_{k}\mathbf{R}^{0}P_{i})^{+}_{m(1,2)}$-fixed complexes at the «*association*» stage (**I***a*⇀) of the two MAL_S(3),(4)-reactions ($\mathbf{I}_{1,2}$)(Figs. 1b, and Figs.2,3,4).

Naturally that the *reverse* process of the «*d*esorption» (↽**I***d*) occurs at the «*dissociation*» stage(↽I*d*, Fig.1b**,** and Fig. 2) with the *reverse* transformation of the fixed two $({}_{k}\mathbf{R}^{0}P_{i})^{+}_{m(1,2)}$–complexes into the free state of the diffusing $P^{+}_{i(3,4)}$-components ($D_{3,4}$>0; principal schemes, Figs.1b).

These two jointly satisfiable «sorption-*association*(⇀**I***a*), and desorption-*dissociation*(↽**I***d*)» stages are presented at the pictorial diagrams of the two MAL reactions (1),(2), (Figs. 1b,and 2) with the corresponding MAL_S relations (3),(4) at Fig. 2(down, *right*). As the result of the co-operative («sorption», **I***a*⇀ where $\mathbf{J}_k$ <0, see Fig. 2, *left* and «*d*esorption»,↽**I***d where* $\mathbf{J}_k$>0, see Fig. 2, *right*) behaviour (i.e. Fig. 2, *left*, and *right*) at the MMT NC $\mathbf{k}^{(2)}$(**6**)-selective system may be presented schematically as the corresponding mass transformations $P^{+}_{(3,4)} \rightleftharpoons ({}_{k}\mathbf{R}P_{i})^{+}_{m(1,2)}$ in the visual diagrams of the Fig. 1b, and Fig. 2.

The two fixed (i.e. $D_{m(1,2)}$=0) «complexes», $({}_{k}\mathbf{R}P_{i})^{+}_{m(1,2)}$ of the principal $m_{1,2}$-components transform to the diffusible free $P_{i(3,4)}{}^{+}$-ionic (sorbate) principal components in the **I**, selective sorption and **II**,multi($D_{3\text{-}5}$)-Diffusion NC selective process expressed via the MAL_S «dissociation» reaction (↽I*d*, Fig. 2, *right*). According to the MAL_S forward «mass transformations» mechanism (3),(4) of the reactions ($\mathbf{I}_{1,2}$) in the *bi*-functional NC Model proposed (see Figs. 1b and Fig. 2) the free diffusing principal $P^{+}_{i(3,4)}$ (sorbate) components are transformed into the two fixed ($D_{m(1,2)}$=0) principal $({}_{k}\mathbf{R}^{0}P_{i})^{+}_{m(1,2)}$ -components. Thus in short schemes $P^{+}_{i(3,4)} \rightleftharpoons ({}_{k}\mathbf{R}^{0}P_{i})_{m(1,2)}$ the reverse two $MAL_{\mathbf{S}}$ mass transformation (3), (4) of the two reactions ($\mathbf{I}_{1,2}$) reduces to the «*d*issociation» stage (**I***d*): $P^{+}_{i(3,4)} \leftharpoondown ({}_{k}\mathbf{R}^{0}P_{i})_{m(1,2)}$ (Fig. 2, (1),(2) reactions, Fig.2up,*left*).

There have been considered previously the same approach in the simple NC Model elaborated previously with the only one MAL reaction ($\mathbf{I}_1$) and (3) for the simple type of the MMT NC $\mathbf{k}^{(1)}$=5 *variance* for the $\mathbf{I}_1$, selective sorption including **II**, Diffusion ($D_{3,j}$) system with only one $P^{+}_{(3)}$-(sorbate) diffusing component [5-8].

It is obvious that the investigation of the interference effects for the two principal diffusing *P* $P^{+}_{i(3,4)}$ -(sorbate) components is not available in the simple MMT **NC** selective system with $k^{(1)}$=5-*variance*[5-8]. The simple MMT NC $\mathbf{k}^{(1)}$(5)-system is characterized by the $k^{(1)}$=5-*variance* number (where the $k^{(1)}$(5)-*variance* is principially the smaller number of the degree of freedom) [5-8]

In this publication there is developed the effectively advanced MMT NC $\mathbf{k}^{(2)}$(**6**)- **I**, selective sorption-desorption plus the II,multi-Diffusion NC system which is characterized by the larger $\mathbf{k}^{(2)}$(**6**)-*variance* in comparison with the another previous simple $k^{(1)}$(5)-variance system [5-8] (where $\mathbf{k}^{(2)} \geq k^{(1)}+1$).

The larger $\mathbf{k}^{(2)}$(**6**)-*variance* corresponds to the larger number of the degree of freedom attained for the multi(6)-component MMT NC selective sorption combined system with the $\mathbf{k}^{(2)}$=**6**-*variance*. The *variance* is known as the principially important integral parameter of the irreversible thermodynamics theory [11-13].

Now for the new advanced MMT NC, $\mathbf{k}^{(2)}$(**6**)-selective combined sorption system (with the two principal $P^{+}_{i(3,4)}$-sorbate components) the previously *unachievable* possibility in the simple $k^{(1)}$(5)-system[5-8] *to*consider such interference effects for the two principal $(P_i)^{+}_{(3,4)}$-sorbate diffusing components as for example D*isplacement* D*evelopments (*DD*)* is now available, and realized successfully here in this publication.

Thus it is attained here (later in **S**.4) the visual computerized new results for the interference of the propagating $X_{m(1,2)}$–concentration waves of the principal $({}_k\mathbf{R}^0P_i)^{+}_{m(1,2)}$-fixed ($D_{m(1,2)}$=0) complexes including the DD effects of the $X_{m(1,2)}$-waves interaction. The computerized calculated DD effects are achieved and displayed in Figs. 3.A, and 4.B (**S**.4). The discussion of the calculated combined bi-functional NC Model including the new results are presented for the propagating $X_{\mathbf{n}}$-concentration waves (**n**=**1**,**2**,…**6**) in S.4 (Figs. 3A,and Figs.4B) obtained by the author's computerized calculations.

In addition there is the important generalized and fundamental remark here, namely the MMT NC kinetics with **I**, selective sorption and **II**,multi-Diffusion, $\mathbf{k}^{(2)}$(**6**)-selective combined system is more variable (due to the two formed fixed principal $({}_k\mathbf{R}^0P_i)^{+}_{m(\mathbf{1,2})}$-components-«complexes»). Due to the enlarged degree of freedom, and to the availability of the two principal $({}_k\mathbf{R}^0P_i)^{+}_{m(1,2)}$-components, i.e. MAL_S-«complexes» ($\mathbf{I}_{1,2}$) the extended $\mathbf{k}^{(2)}$(**6**)-*variance* of the NC $\mathbf{k}^{(2)}$-systems provide the principal advantage in comparison with the previously considered [5-8] simple $k^{(1)}$(5)-components bi-functional NC MMT sorption systems.

The generalized phenomenological mathematical technique is described here below (in S. **4**) on the basis of the non-equilibrium thermodynamics approach[1-4,11] via the mathematical partial differential mass transfer **n**-Eqns (3.3) [8, p.762], which have been using together with the proposed and advanced *bi-functional* properties for the advanced NC selective Model with $k^{(2)}$-**I**, selective combined «sorption-desorption» (1),(2)equations, and **II**, multi-($D_{3\text{-}5}$) Diffusion implemented (i.e. **I**, Selectivity)&(**II**, multi-Diffusion)-MMT routes).

The conceptual scheme of the bi-functional NC $\mathbf{k}^{(2)}$-Model (Figs**.**1a,b, and Fig.2) clarifies the details of the *bi-functional* NC Model with the two routes, i.e. $\mathbf{I}_{1,2}$ -route with ((1),(2)) reactions including the two component $\{K_S^{1},K_S^{2}\}$-Selectivity factor determined by the (3),(4)MAL_S relationships including the Diffusion **II**, route with the $\mathbf{\{}D_{\mathbf{3,4,j5}}\mathbf{\}}$-multi-Diffusivity. Such *bi-functional* NC Model is implemented into the mass transfer partial differential **n**-Eqns systems mentioned [8] (see the description of the process of the MMT bi-functional **NC** kinetics[1-8].

Here the advanced MMT selective sorption combined **NC** Model with the $\mathbf{k}^{(2)}$-variance is presented via the generalized conceptual scheme (Fig.1b, and Fig. **2**) including the all vectorial internal $\mathbf{J}_{,m(1,2),,\mathbf{k}}$-mass fluxes (see Fig. 2) for the diffusing two principal $P^{+}_{i(3,4)}$-sorbate components mentioned earlier.

The $\mathbf{J}_{m(1,2),\mathbf{k}}$-mass fluxes are determined as the internal fluxes as they are expressed by the MAL_S relationships (3**);(**4),$\{K_S^{1};K_S^{2}\}$via the Selectivity $\mathbf{I}_{1,2}$-route, (see (1),(2) and Figs. 1b**,** 2) including the two MAL_S relations **(**3),(4))[1-4,8]. The generalization of the **NC**, MMT kinetics process is realized by the inclusion into the consideration of the additional internal $\mathbf{J}_{m,\mathbf{k}}$- mass fluxes which are expressed by the «sink» (*forward*, **I***a*⇀)&»source»(*backward*, ↽**I***d*) mechanism for the $\mathbf{J}_{\mathbf{k}}$-mass flux along the co-route $\mathbf{I}_{1,2}$ (Fig.2)**.** Figure. 2 displays the sink **I***a* (*left*)–source **I***d* (*right*) source - mass transfer mechanism, where the $\mathbf{J}_{k,m,i}$ – the all mass fluxes.

Two theoretical basic, and key common concepts are used in the study of the both, MMT $k^{(1)}$[6,7], and $\mathbf{k}^{(2)}$–selective combined (**I**, selective sorption and **II**, multi-Diffusion) NC systems here with the obvious advantage of the $\mathbf{k}^{(2)}$(**6**)- **I**, NC system mentioned (**I**,selective sorption and **II**,multi-Diffusion).

The fundamental well-known (in the irreversible thermodynamics, [1-4,12-14]) «**W**ave concept» (denoted here and previously as $\mathbf{W}^{+}$[1-8,10,13]) of the multicomponent interactive $X_{\mathbf{n}}$-concentration waves (**n**=**1**,**2**,...$\mathbf{k}^{(1,2)}$) propagating in the *bi-functional* NC **L**-matrices for the MMT kinetics process of the $\mathbf{k}^{(1,2)}$-components mixture (**n**=1,2,3,4,5, $\mathbf{k}^{(2)}$=**6**).

In this publication there is considered the MMT, NC process for the advanced $\mathbf{k}^{(2)}$=**6**-selective combined system inside the planar NC L-membranes. The NC MMT process for the any **n**-components of the $\mathbf{k}^{(2)}$-component mixture (**n**=1,2,..,5, $\mathbf{k}^{(2)}$) is considered for the case when the appearing, and interactive $X_{\mathbf{n}}$(L-distance;**T**-time)-concentration waves propagate in the course of time (**T**) inside the **NC** matrix from the contact: «**NC** surface/external solution» (Fig.1b, on the *right*) into the separate selective route (**I**)at the NC sorbent L-membrane (see also Figs. 3A, and 4B), i.e. $X_{\mathbf{n}}(L;\mathbf{T}^{1,3})$-distributions; **S**.4). The additional significant explanatory computerized visual results with the illustrations (Figs.3A and 4B are represented below in **S**.4).

The multi-component $X_{\mathbf{n}}(L,T)$-concentration waves for the MMT selective NC combined systems ($\mathbf{I}_{1,2}$; **II** routes for the mass transfer process) propagate in the full analogy with the MMT in the theory of multicomponent frontal chromatography. The difference between the two variants of the MMT processes mentioned concludes in the availability of the linear velocity for the column chromatography. The difference between the character of the particular $X_{m(1,2),k}$ -waves in the NC MMT process and the usual $X_{\mathbf{c}}$-concentration waves in the multicomponent chromatography will be discussed later.

Figures 1b display the input vectorial external diffusion $\mathbf{J}_{,(3,4)p,\ j5}$- mass fluxes(Fig.1b, white arrows, *right*) together with the internal $\mathbf{J}_{\mathbf{k,m}}$-mass fluxes (Figs.1b, coloured vertical arrows) of the masses of the **n**-components of the new MMT advanced $\mathbf{k}^{(2)}$(**6**)-selective NC combined (**I**, selective sorption and **II**, multi-Diffusion) system.

Figure 2 displays visually the details including the resulting $\mathbf{J}_{k,i,m}$-mass fluxes of the mass transfer «sink-source mechanism» (Fig. 2, *down*) which explains its action during «desorption» (I*d*) and «adsorption» (I*a*) stages (Fig. 2 in the *middle*). The extended detailed explanation in the text are presented by the Fig. 2 in the last recent publications [1-4,10].

Displacement Development in Concentration Waves Behaviour for combined NC Sorption System

There were included all the Equations (**S**.3) for the $\mathbf{6}^{th}$-component **NC** MMT $\mathbf{k}^{(2)}$(**6**)- **I**, selective sorption and **II**,multi-Diffusion -sorption system previously presented including the two principal components, namely two principal «sorption-desorption» relations (1),(2) $({}_{k}\mathbf{R}^{0}P_{i})^{+}{}_{m(1,2)}$, ($m_{\mathbf{1,2}}$-fixed and in diffusible «complexes» where $D_{m(1,2)}$=0), and besides two principal ($D_{3,4}$>0)-diffusible «free» principal $P^{+}{}_{i(3,.4)}$-components**.** The sorptive power of the bi-functional NC for the $P^{+}{}_{i(3,.4)}$-sorbate components are characterized by the two component Selectivity $\{K_S{}^{1}(3);K_S{}^{2}(4)\}$- factor according to the two MAL_S relationships (3),(4) determined at Fig. 2).

The numerical technique is based on the implicit finite difference formulation (with the *forward* and *reverse* mathematical sweeping procedures) for the generalized parabolic partial difference diffusion mass balance **n**-Eqs. (3.3)[8, (3.3)] with the iteration technique

including the multicomponent mathematical matrix calculations approach, and the multi-component mathematical matrix inversions.

On the mathematical basis [1-8] of the (*FORTRAN*) computer programs were elaborated and arranged for the numerical schemes with inclusion of the partial differential **n**-Eqns. mentioned and the MMT combined NC process were constructed [1-8]. First the simple combined MMT process on the basis of $k^{(1)}$-variance NC Model was modeled [5-7].

For the considered case of the new advanced $\mathbf{k}^{(2)}(\mathbf{6})$-NC Model the new advanced computerized program have been modernized. The approximate numerical computerized solution of the MMT partial differential Eqns (3.3)[8] was carried out for the six component ($\mathbf{k}^{(2)}=\mathbf{6}$) in the **NC** matrix with the inclusion of the **D**iffusion relationships for the concentration $\{X_{\boldsymbol{\epsilon}}\}$ and electrical $\{\boldsymbol{\Phi}\}$ fields influence [5,11].

Usually as a rule the «Displacement» effect is discussed widely as the chromatographic one for the sorption phenomena [13,15-17].

It is known that the DD chromatographic effect is the results of the interference of the two propagating sorption $\{X_{\mathbf{n}}\}$-concentration waves, namely the second X_2-concentration wave displaced. The X_2-concentration wave (for the less selective 2-component with the $K_S^{\mathbf{2}}$-selectivity) is displaced by the more selective $X_{\mathbf{1}}$-concentration («displacer») wave of the more selective **1** (K_S^{1})-«displacer» $m_{\mathbf{1}}$-component (where $K_S^{1}>K_S^{2}$)in the sorption medium.

Figures 3,4 display visually the DD effect with the aid of the *L*-spatial propagation of the $X_{\mathbf{1,2,6}}(\boldsymbol{L},\mathbf{T}^{\mathbf{1,3}})$-concentration waves in the course of $\mathbf{T}^{\mathbf{1,3}}$-time. The part of the calculated new results of the author's numerical modeling is presented in Figs. 3A and 4B.

The presentation of the propagation of the computerized $\{\mathbf{X_n}(\boldsymbol{L},\mathbf{T})\}$-concentration waves may be presented additionally (including the previous modeling author's results [1-8,15-17]) in the more acceptable and visual presentation mode named here as the **S**cientific **C**omputerized **A**nimations-video files. Such visual approach (or in other words as the computer-generated imagery «SCA.*avi*»-video files) is used by the author of this publication [2-5,15-17].

The picture frames in the SCA**.***avi* video files are represented by the computerized multi-colored multi-component $\{\mathbf{X_n}\}$-frames positioned in the ascending order for $\mathbf{T}^{S}$-times ($T^0<T$). The visual examples of the computerized several «picture-frames» (used for the «SCA**.**avi» video-files) are displayed here in Figs. 3A and 4B. The explanation of the meaning of the multi-component (multi-colored) wave «picture-frames» (in Figs.3A and 4B) is given *below*. The «SCA.*avi*» examples are included and used permanently by the author during the oral presentations at many international conferences and seminars [1-8, 15-17].

The visual demonstration of the *bi-functional* **NC**, MMT kinetics during the oral author's presentations are prepared via the «SCA.avi» video-files as the results of the computerized mathematical modeling via the propagating $\{X_{\mathbf{n}}\}$-concentration multi-colored waves calculated finally. Then the calculated frames are arranged for the successive time moments(T^S) in the «SCA.*avi*» video-files produced [1-8,15-17]. The corresponding «SCA.*avi* video files» demonstrated clearly are perceived by the sci. audience [1-8, 15-17] easily.

Here (in **S**.4) the computerized results are displayed in the more simple manner (as the multi-colored «picture-frames», in Figs.3A and 4B) than in the visual «**SCA**nination» method mentioned above. The complete set of the separate two $\{X_{\mathbf{n}}(L,\mathbf{T}^{\mathbf{1,3}})\}$ multi-colored «picture-frames» display the behavior of the advanced propagation of the $X_{\mathbf{1-6}}(L,T)$-concenration waves (for the current $\mathbf{T}^{\mathbf{1,3}}$-time moments). The propagation of the multi-colored $\{\mathbf{X}_{m(1,2)}, X_{\mathbf{k(6)}}(\boldsymbol{L},\mathbf{T}^{\mathbf{1-3}})\}$-concentration waves happens (from *right*, $\boldsymbol{L}=1,T^1$ to *left*, $\boldsymbol{L}=0,T^3$) for the two various A,B-variants (Figs.3($A.T^{1,3}$) and 4(B, $T^{1,3}$)). The A,B variants

differ in the various values of the two component $\{K_S^1, K_S^2\}$-Selectivity factors (Figs. 3A, and 4B).

The each of the computerized A,B-variants are calculated and displayed visually (Figs.3, variant A, and Figs.4**,**variant B) for the following parameters introduced, namely two component $\{K_S^1; K_S^2\}$-Selectivity factor; three$\{D_{3,4,5}\}$-Diffusivity values and then the set of the input $\{X_{\mathbf{n}}^0\}$-waves concentrations (examples in Figs captions of Figs.3A and 4B). The propagation of the *particular* multicomponent $X_{\mathbf{L}1,2,\mathbf{6}}(\mathbf{T^{1\text{-}3}})$-concentration waves**(**where$\{D_{\mathbf{1,2,6}}=0\}$**)** are displayed in the course of the discrete $\mathbf{T^{1,3}}$-times values in the ascending order i.e. $\mathbf{T^3}$=12(left); $\mathbf{T^1}$=3(*right*); at Figs 3A and $\mathbf{T^3}$=18(left); $\mathbf{T^1}$=6(*right*) at Figs. 4B.

Figures 3A, and 4B display the direction of the propagation of the advancing $\{\mathbf{X}_{1,2,6}\}$-concentration waves across the **NC** L-membrane from its *right* side (***L***=1) to its *left* side (***L***=0) (see Figs.1b, and Figs.3A;4B). Thus Figs.3A,4B display the propagation of the three particular$\{\mathbf{X}_{1,2,6}(\boldsymbol{L},\mathrm{T})\}$-concentration waves in the NC L-matrix for the fixed and indiffusible $m_{1,2}$, and $\mathbf{k}^{(2)}(\mathbf{6})$-components (with zero Diffusivities, $D_{1,2,6} = 0$).

These propagations of the $m_{1,2}$; $\mathbf{k}^{(2)}(\mathbf{6})$-waves through the L-membrane occur to the *left* side (***L***=0, Fig.1b) from the *right* side (***L***=1)(see the black arrow to L=0⬅ in Fig.1b). The direction (to the *left* side from the *right* side of the L-membrane) for the all $\{X_{\mathbf{n}}(L,\mathrm{T})\}$-concentration waves ($\mathbf{n}$=**1**,**2**,…$\mathbf{k}^{(2)}(\mathbf{6})$) is displayed by the *black* arrows (⬅) in Figs**.**3A, and 4B.

One of the most principal and *integral* $\mathbf{X_6}$-concentration wave (*dash-dotted*) demonstrates the typical «S»-shape during its propagation (see **6**-curves in all Figs. 3A**;** 4B). The particular and *integral* ${}_{\mathbf{6}}\mathbf{R}^0$-wave characterises the particular, and fixed ($D_{\mathbf{k}}$=0) $\mathbf{k}^{(2)}(\mathbf{6})$-component («nanosites», Figs. 1a,b).This ${}_{\mathbf{k(6)}}\mathbf{R}^0$-component was deliberately declared and introduced at the initial (and key) stage of the creation of the author's **NC** Model elaborated for the **NC** MMT $\mathbf{k}^{(1,2)}$-sorption combined systems. The corresponding remark for the significance of the ${}_{\mathbf{k(6)}}\mathbf{R}^0$-component («nano-sites») is presented especially, **S**2)[1-8].

During the mathematical computerized modeling of the MMT **NC** process with the results displayed in Figs. 3A, 4B there was calculated the well known *integral* parameter - **C**entre of **M**ass (or $\mathbf{CM}(\mathbf{T^{1,3}})$) for the *integral*${}_{\mathbf{6}}\mathbf{R}^0$-concentration distribution of the $\mathbf{k^{(2)}(6)}$-wave. During the computerized modeling the **CM**(T)-values calculated are close to the $\boldsymbol{L}_{\mathrm{mx}}^{1,3}$-positions for the concentration maximums ($\mathbf{X_2^{mx}}(\mathbf{T^{1,3}})$)at any current $\mathbf{T^{1,3}}$-times values.

Thus the **CM** (**C**entre of **M**ass) of the integral ${}_{\mathbf{6}}\mathbf{R}^0$-concentration wave supports its physical meaning. The **CM**-value of the *integral* ${}_{\mathbf{k(6)}}\mathrm{R}^0$–concentration wave (varianve, $\mathrm{k}^{(\mathbf{2})}$=**6**) is close to the $\boldsymbol{L}_{\mathrm{m}}^{1,3}$-«positions» of the concentration maximums-$X_2^{\mathbf{mx}}(\mathbf{T})$ of the displacing 2-principal m_2-component-complex. Consequently during the MMT NC process the **CM**-values are almost equal to the $L_{2\mathrm{m}}$-positions. In such a way the *integral* $\mathbf{CM(T^{1,3})}$-values «indicate» the results of the DD-Effect, namely the $\boldsymbol{L}_{2\mathrm{m}}$-positions in Figs. 3A and Figs**.** 4B.

Let us look at the propagation to the *left* (L=0) ⬅ from the *right* (L=1) of the NC L-matrix (see the wave's propagation along the black arrow at Fig. 1b, *up*) of the specific $X_{\mathrm{m}(1,2)}$-concentration waves for the fixed $m_{1,2}$-components, Fig. 3A (T^3=12>T>T^1=3), and Fig.4B (T^3=18>T>T^1=6).

Thus it is obvious that the NC MMT kinetics process at Fig. 3A (large K_S^{1A}=400) is much faster than the kinetics process at Fig. 4B (moderate K_S^{1B}=320). The same dependence takes place for the DD effect value ($X_2^{mx\text{-}}$ peak amplitude of X_2-concentration), namely(compare Figs.3A and Figs.4B):

X_{2A}^{mx}(Fig.3A, K_S^{1A})=0.65 > 0.52=X_{2B}^{mx}(Fig.4B, K_S^{1B}), where K_S^{1A} >K_S^{1B}

Inside the NC matrix there are presented the fixed components (such as free «integral» nano-sites $_{\mathbf{k(6)}}R^0$-wave profile (6-curve) which have zero Diffusivity, D_6=0. Naturally that the immovable$(_k\mathbf{R}^0P_i)^+_{m(1,2)}$- fixed «complexes» have no diffusion mobility ($D_{(1,2)}$=0) also.

Nevertheless the particular{$\mathbf{X}_{(1,2),}$and $\mathbf{X_6}$}-concentration waves propagate in the *bi-functional* NC matrixes.[1-8]. The distinguishing feature of the $m_{1,2}$-waves consist of the «$(_k\mathbf{R}^0P_i)^+_{m(1,2)}$-in diffusible «complexes» (with zero Diffusivities, $\mathbf{D}_{m(1,2)}$=0).

The influence of the two component {K_S^1;K_S^2}-Selectivity factor on the propagation behavior of the {$X_{1,2,6}$}-concentration waves displays here in Figs. 3A, and 4B. Both Figures 3A and 4B illustrate the influence on the {$X_{1,2,\mathbf{6}}$}-concentration waves behavior of the various sets of the determining factors, namely-{$D_{\mathbf{3\text{-}5}}$}-Diffusivities; {X_n^0}- input concentrations values. The particular $X_{m(1,2)}$-concentration waves interference includes the DD effect displaying the peak with the $X_{\mathbf{2}}^{mx}(\boldsymbol{L}_{2m})$-dependence for the X_2^{mx}-maximums of 2-component concentrations (Figs.3A; 4B). All the ($X_{1,2,\mathbf{6}}(\boldsymbol{L},\mathbf{T})$-concentration values are the results calculated by the computerized modeling mentiontd.

The DD effect occurs as the result of the interference between the two particular$X_{\mathbf{1,2}}$-concentration waves. Thus the X_2-concentration wave is displaced by the *incursion* of the another $X_{\mathbf{1}}$-concentration wave of the «displacer» (namelyX_1-wave of the 1-component-displacer with the $K_S^{\mathbf{1}}$-Selectivity). The DD-effect is determined by the two component {K_S^1,K_S^2}-Selectivity factor in the MAL_S relationships ((3),(4), and Figs. 1b, 2 (with the large Selectivity «K_S^{1A}=400» for the «displacer», and K_S^{2A}=50 for the 2-component displaced, Figs. 3A. Figures 4B display the influence of the moderate displacer «$K_{S\mathbf{1}}^B$=320» in two component **S**electivity^B{$K_S^{\mathbf{1}B}$=320, K_S^{2B}=40} factor.

The comparison between the various - K_S^{1A}(400, Figs.3A), and K_S^{1B}(320, Figs. 4B) values (where $K_S^{1A}>K_S^{1B}$) shows in details the more essential influence of the DD -effect for the large K_S^{1A}(400)-Selectivity value (see Figs. 3, from $\mathbf{T^1}$(*left*) to $\mathbf{T^3}$(*right*) in comparison with the influence of the moderate K_S^{1B} (320)-value in the case of Figs.3 (comparison between Figs. 3A and Figs. 4B).

T^3=12 ; X_2^{mx}=0.58 T^1=3 ; X_2^{mx}=0.61

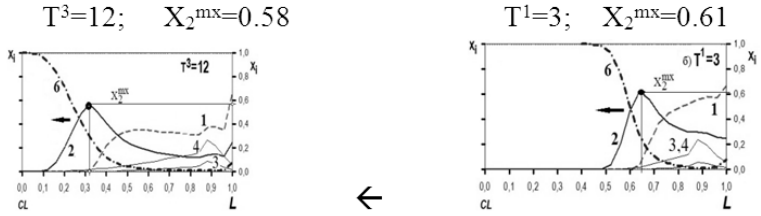

(*left*, T^3=12); L_{2m}=0.32; (*right*, T^1=3); L_{2m}=0.65

(*left*, T^3=12); L_{2m}=0.32 (*right*, T^1=3); X_{2m} =0.65

Fig. 3. (T^3-T^1) Variant A($\mathbf{K_S}^{(1,2)A}$=400;50**).** DD effect for $X_{1,2,\mathbf{6}}(L,\mathbf{T})$-concentration waves in NC L-membrane: **1**-displacer, (dashed); **2**-displaced,(solid);3,4-thin lines; **6**-«integral» wave ($_kR^0$-(dash-dotted). (horizontal movement of **1-6-concentration** waves*:* (*to left,*$\mathbf{T^3}$=12)←(from *right,*$\mathbf{T^1}$=3, *see* Fig.1b) for kinetics displacement through NC L-membrane, depending on two governing factors: Selectivities {$K_S^{1,2}$} and input concentrations {$X^0_{1,2}$}-values: $K_S^1(400)^A>K_S^1(320)^B$. Diffusion coefficients: {$\mathbf{D}_3$=0.1; $\mathbf{D}_4$=0.055;$\mathbf{D}_5$=0.02}^{A,B}. All values are dimensionless. T^3=18 ; X_2^{mx}=0.50 T^1=6 ; X_2^{mx}=0.52

The DD effect is well known as the chromatographic effect. The reason of the DD effect in theory of chromatography is the difference between the $K_S^{1A,B}$-Selectivity values. The analogy between the NC MMT kinetics and Theory of the Multicomponent chromatography is especially emphasized in the author's publications [1-4, 15-17].

Therefore it is important to consider the details of the DD effect in the **NC** MMT kinetics investigation here. Figures 3 and 4 give an opportunity to present the $\mathbf{k}^{(2)}$(**6**)- NC

Model for the investigation of the details of the DD effect in the MMT $\mathbf{k}^{(2)}(\mathbf{6})$- NC sorption systems.

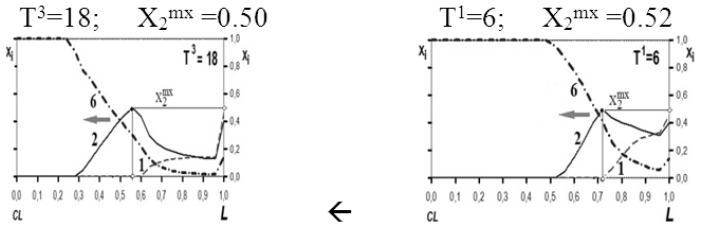

(*left*, T^3=18); L_2m=0.55; (*right*, T^1=6); L_2m=0.

(*left*, T^3=18); L_{2m}=0.55 ← (*right*, T^1=6); L_{2m}=0.71

Fig. 4. (T^3-T^1) Variant B**.** ($\mathbf{K_S}^{(1,2)B}$=320;40)**.**DD effect for $\mathbf{X_{1,2,6}}(L,\mathbf{T})$-concentration waves in NC L-membrane: 1-displacer, (dashed) ; 2-displaced,(solid); **6**-«integral» wave ($_{\mathbf{k}}R^0$- (dash-dotted). (horizontal movement of 1,2,6 waves*:* (*to left*,$\mathbf{T^3}$=18)←(from *right*,$\mathbf{T^1}$=6, *see Fig*.1b), for kinetics displacement through NC L-membrane, depending on two governing factors Selectivity's ($K_S^{1,2}$) and input concentration $\{X^0_{1,2}\}$ values: $K_S^{\mathbf{1}}(400)^{\mathbf{A}}>K_S^{\mathbf{1}}(320)^{\mathbf{B}}$. $X_{i(3,4)}(L,T)$-waves are omitted (to make the pictures clear). All the values are dimensionless.

The propagation of the distinctive $X_{1,2,\mathbf{6}}(L,T)$-waves for the MMT NC $\mathbf{k}^{(2)}(\mathbf{6})$-system (see Figs. 3A;4B(T^3, *left*; T^1,*right*) is determined by the main characteristic parameters of the MMT NC kinetics: (***1***) two component $\{K_S^1;K_S^2\}$-factor, for the fixed $m_{1,2}$-principal components and

(***2***) multicomponent $\{D_{3\text{-}5}\}$-Diffusion factors for the mobile principal $P^+_{i(3,4)}$- components, and finally

(***3***) - two input concentrations $\{X_{(3,4)}{}^0, L=1\}$ at the input of the L-membrane (at L=1, *right*, Figs.1-4).

The remaining input concentrations data are determined by the conditions of the (1),(2)- NC sorption equilibria: $_mX_{1,2}{}^0$ for the $(_k\mathbf{R}^0P_i)^+_{1,2}$-«complexes» due to the two MAL_S (3**)**.(4)-relations, and due to the condition of the constancy for the initial $_{\mathbf{k(6)}}\mathbf{R}^0$-concentration inside the NC L-matrix:

$$[_{\mathbf{6}}R^0]^0 + [(_k\mathbf{R}^0P_i)^+_{m1}]^0 + [(_k\mathbf{R}^0P_i)^+_{m2}]^0=1 \qquad (4.1)$$

The remaining $\mathbf{j}_{(5)}$-co-ion $\mathbf{X}_{j(5)}$-concentration is determined from the obvious *electroneutrality* condition: $[(X_5{}^0)^-]^{negative}=X_1{}^{0+}+[X_2{}^{0+}]^{positive}$. The diffusion $\{X_{3,4,5}\}$-concentrations waves are calculated during the computerized numerical modeling mentioned but not displayed in Figs. 3A and 4B knowingly for not encumbering the main results concerning the propagation of the particular $\{\mathbf{X}_{m(1,2)},\mathbf{X_6}\}$-concentration waves.

The part of the results of the computerized modeling and investigation is calculated and presented visually by the frames-pictures at Figs. 3A and 4B. The various governing parameters for the combined MMT NC process: $\{K_S^{1,2}\}$ together with the input $\{X^0_{1,2}\}$-concentrations of the combined MMT kinetics process are presented at the Figs. captions 3A and 4B.

Conclusions

Displacement Development (DD) concentration waves during multicomponent Mass transfer in Sorbents-NanoComposites

1. The computerized results for the propagation of the *particular*$\{X_{\mathbf{1,2,6}}\}$-concentration waves is determined by the decisive influences of the combination for the two MMT routes, namely $\mathbf{I}_{1,2}$ **-**, Selectivity, and **II**-multi-Diffusion -parameters:

I$_{1,2}$-Selective MMT *Route*. **{**K_S^1;K_S^2**}**-Selectivity effects (MAL_S for sorption at the $_kR^0$-nano-sites; two Selectivity parameters for the two *principal* $m_{1,2}$-components-«m-complexes»- $(_k\mathbf{R}P_i)^+_{m(1,2)}$ route, **I**, **(**Fig. 2**).**

II–Diffusion MMT *Route*. {$D_{i(3,4)}$; D_{j5}}-multi-diffusion effects:$\mathbf{D}_{(3,4)5}$: diffusible $P_{i\ (3,4)}$ - principal components, including co-ions diffusion ($\mathbf{D}_5$-diffusing j_5-co-ions).

2. The propagation of the special *integral* $_{k(6)}\mathbf{R}^0$-concentration wave in the *bi-functional* **NC** matrix in the course of **T**-time takes place, although the corresponding $\mathbf{D}_k$-diffusivity is zero ($\mathbf{D}_{k(6)}$=0). The two particular $X_{m(1,2)}$-concentration waves propagate in the same way (where $D_{1,2}$=0) like $_{k(6)}\mathbf{R}^0$-wave. All the results of the computerized modeling (**S**.3,4) are displayed visually by the picture-frames of the SCA.avi animations (Figs.3a,b and 4a,b, **S**.4) taken from the computerized «SCA.avi» video-files.

Such atypical (*unusual*) integral $_k\mathbf{R}^0$-concentration wave (k**(6)**-curve, *dash-dotted*, Figs.3 and 4), including the two $\mathbf{X}_{m(1,2)}$-concentration waves (**1,2**-curves) behavior has the clear physical meaning. The diffusion propagation of the *integral* $_k\mathbf{R}^0$-wave, and the particular $X_{m(1,2)}$-concentration waves are determined by the combined behavior of the diffusible $P_{i\ (3.4)}$- principal components which includes the *combined* $P^+_{i\ (3.4)}$-participation in the two co-operative processes: namely in the $P^+_{i\ (3.4)}$- «mass transformation» (via the co-route $\mathbf{I}_{1,2}$) in *combination* with the{$\mathbf{D}_{(3,4)}$}-multi-diffusion in the **NC** pores (via the co-route **II**, $\mathbf{D}_{j,(3,4)}$>0).

The corresponding author's conceptual schemes for the *bi-functional* NC $\mathbf{k}^{(2)}$**(6)**-Models (Figs. 1a,b; S.2) displayed distinctly the *combination* of the two MMT co-routes (**I**&**II**, see comments here (above).

Visualization of the propagating concentration waves behavior by the SCA.avi animations

The computerized variants of the MMT $\mathbf{k}^{(2)}$**(6)**-sorption **NC** system including the new theoretical numerical results for the *particular*{$\mathbf{X}_{m(1,2)}$(*L*,T)}-concentration waves behavior are *visualized* by the author via the contemporary method of the computerized *visualization* of the simulation results, namely via the multi-colored computerized SCA-animations (i.e. «SCA.avi» multi-colored video-files).

The «SCA.*avi*» video files are assembled sequentially via the separate multi-colored «pictures-frames» arranged in course of **T**-time. Such separate frames of the «SCA» are displayed in Figs. 3A, and 4B as the usual «animation pattern» [10]. The scanning computerized «SCA.*avi*» files are executed within the many oral author's presentations for the MMT NC process. For the publication considered the computerized SCA**.***avi* video-files demonstrate the Displacement Development (DD-effect) during the animated propagation of the multi-component (and «multi-colored») {X_n}-concentration waves in spatial coordinates (*L*-distances, Figs. 3A; 4B) in the course of **T**-time during the MMT **NC** processes for the modern advanced **NC** Model of the $\mathbf{k}^{(2)}$**(6)**- multi-variance sorption combined NC system inside the *bi-functional* NC **L**-matrix.

Such multi-colored SCA-demonstrations (via the «SCA.avi» video file) of the MMT NC processes are well perceived during the oral computerized presentation (at the conferences and seminars in particular). These *visualizations* are perceived, and well understandable by the sci. audience. The considered «SCA.avi»-method of visualization has been used permanently for the implementation of the «SCA.*avi» video*-files into the various author's oral thematic presentations of the MMT **NC** kinetics and dynamics process in the $\mathbf{k}^{(1,2)}$-sorption systems.[1-8]

The multi-colored computerized SCA**.**avi animations (as the «SCA.avi» video files prepared) have been used by author of the manuscript with the permanent experience in the

effective and visually perceptible presentations of the **NC** MMT kinetics processes[1-8] (and of the MMT dynamics previously [15-17]) in many International Conferences (including in particular the well known Conferences «IEX 2004, 2008, 2012», Cambridge, UK).[15-17]

Highlights: a. Computer simulation by the mass balance Eqns. includes the advanced recent Nano–Composite (NC) Models. b. Results of the numerical computerized solution bring the propagating mode of the multi–X_n(L,T)concentration waves inside NC. c. Phenomenological wave W–concept is extended to a sorption transport phenomena in the NC (NanoComposites) sorbent. d. Calculated *visual* animations SCA,avi video-files show the interference of concentration waves for n-components. e. Simulation results show *visually* the chromatographic Displacement Developments (DD) in the NC via the wave W–concept. e. Displacement Development occur during the mass transports visualized for the sci.audience via the «SCA.avi» animations constructed by a computer program. f. The MMT transport through the bi-functional NC matrix leads to the propagation of the particular 1,2,k(«nanosites»)-concentration waves behavior.

References

1. Kalinitchev A., *Prot.Met.&Phys.Chem. Surf.* (Springer Ed.), 2019, Vol. 54(6), Eng. (Rus.) accepted (in print).
2. Kalinitchev A., *Journal for Phys. Chem.*(Rus.), 2019, No 9, pp.369-377. doi: 10.1134/S0044453719090073.
3. Kalinitchev A., *Sorbtsionnye i khromatograficheskie protsessy*, 2018, Vol. 18, No 5, pp.916-930.(Rus).
4. Kalinitchev A., *Material Sci & Eng.J* MS&EIJ *(USE, Med Crave Ed.),* 2018, No 2(4), pp. 128-132. (CrossRef; doi: 10.15406/mseij.2018.02.00045).
5. Kalinitchev A., *NanoTechnol Rev.*(NTREV). Special issue (N5*) «NanoTechnology: from Convergence to Divergence»*, DeGruyter Ed.**3**(5), 2014, pp. 467-498 (.http://degruyter.com/new/ ntrev2014.3 issuefiles. doi:10.1515/ntrev-2014-0007. Publ. on line 8.10, and Printed 14.10. 2014(Ed. Ja S.Lee).
6. Kalinitchev A., *Prot. Met.&Phys. Chem. Surf.* (Springer Ed.), 2013, Vol. 49(6), pp.627-638. doi:10.1134/S2070205113060051.http: //www. springerlink. com/ openurl. asp?genre =article& ID.
7. Kalinitchev A., *Advances in Nanoparticles*, AnP. 2013, No 2(2), pp. 1-13. Sci.Res.Publ.:SCIRP. E-Journ. doi:10.4236/ anp.2013.22028 (Site AnP:http:// www.scirp. org/ journal/anp/).ID: 31894.
8. Kalinitchev A., *Sorbtsionnye i khromatograficheskie protsessy*, 2016, Vol. 16, No 6, pp.748-768 (Eng).
9. Kravchenko T.A., Polyanskiy L.N., KalinichevA.I., Konev D.V., Nano Kompozity Metall–IonoObmennik. M., «Nauka», 2009, 390 p. (Monografiya) (Rus.).
10. Kalinitchev A. Laboratory and production (Rus), 2019, No 2(6), pp.162-167 DOI: 10.32757/2619-0923.2019.2.6.162.167. http: //labpro-media.ru/wp-content/uploads/2019/05/ Kalinichev.pdf.
11. Haaze R., Termodinamics of Irreversible Processes, (Rus.) Ch.2;4, M., Mir, 1967, 544 p.
12. Helfferich F., Klein G., *Multicomponent Chromatography. Theory of Interference*, New York, M. Dekker Inc., 1970, 360 p.
13 Kalinitchev A., *J. Rus. Chem.* Reviews, 1996, Vol. 65, pp. 95-115. (English) doi:10.1070/RC 1996v065n02A BEH000201.
14. Whitham G., *Linear and Nonlinear waves*, Wiley. NY, 1974, 636 p.
15. Kalinitchev A.I., Hoell W.H., *Ion Exchange Technology for Today and Tomorrow*, Cox M., Ed.,Soc.Chem.Ind.(SCI)Lond., 2004, pp.53-58 (Extend.Thes., pp.349-356).www. soci.org.
16. Kalinitchev A.I., Hoell W.H., *Recent Advancesin IEx Theory&Practice*, Cox M., Ed.Soc.Chem.Ind. (SCI), Lond., 2008, pp. 85-93, (www.soci.org.).
17. Kalinitchev A.I., In «IEX2012» Cox M.,Ed.,Soc. of Chem. Ind., Lond., S. Fundam.(El. Book). 2012. pp. 1-18.

Калиничев Анатолий Иванович – д.х.н. (физ. химия), гл. научный сотрудник Института физ химии и электрохимии им. акад. А.Н. Фрумкина РАН, Москва.

Kalinitchev Anatoliy I. – Doctor Habilitat (Phys. Chem.), principal investigator, Institute for Phys Chemistry and ElectroChemistry named after acad. A.N. Frumkin. RAS (Moscow). E-mail: kalina@phyche.ac.ru